

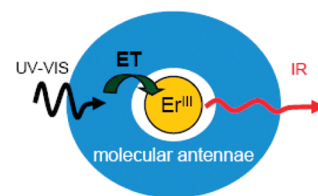
# Population Saturation in Trivalent Erbium Sensitized by Organic Molecular Antennae

Francesco Quochi,<sup>\*,†</sup> Flavia Artizzu,<sup>‡</sup> Michele Saba,<sup>‡</sup> Fabrizio Cordella,<sup>§</sup> Maria Laura Mercuri,<sup>‡</sup> Paola Deplano,<sup>‡</sup> Maria Antonietta Loi,<sup>§</sup> Andrea Mura,<sup>†</sup> and Giovanni Bongiovanni<sup>†</sup>

<sup>†</sup>Dipartimento di Fisica and CGS, Università di Cagliari, SLACS-INFM/CNR I-09042 Monserrato (CA), Italy, <sup>‡</sup>Dipartimento di Chimica Inorganica e Analitica, Università di Cagliari I-09042 Monserrato (CA), Italy, and <sup>§</sup>Zernike Institute for Advanced Materials, University of Groningen NL-9747 AG Groningen, The Netherlands

**ABSTRACT** We investigate sensitization efficiency of near-infrared emission and population saturation of trivalent erbium in erbium–quinolinolato complexes photoexcited into the absorption band of the organic sensitizer. At low-excitation levels, we find high (~80%) sensitization efficiencies. We observe excited-state population saturation at inversion threshold under subnanosecond pumping at the level of one injected photoexcitation per complex.

**SECTION** Kinetics, Spectroscopy



The increasing demand of larger bandwidth in a local area network can be met by adopting novel optical technologies with cost-effective materials. Molecular materials hold great potential in this context. The high processability of molecular materials, combined with the large tunability of their optical properties, have boosted a rapid development of low-cost photonic systems, e.g., optical waveguides and routers.<sup>1</sup> Near-infrared organic light-emitting diodes have also been demonstrated.<sup>2</sup> In these devices, emission takes place from trivalent erbium (Er<sup>III</sup>) ions coordinated to organic molecules (ligands) to form coordination complexes.<sup>3</sup> Erbium complexes can also be exploited as gain materials for signal regeneration in the third telecom band at 1.54  $\mu\text{m}$ .<sup>4</sup>

Population inversion in Er<sup>III</sup> is typically achieved only by intense laser pumping, owing to the low absorption cross-section of Er<sup>III</sup> 4*f* intrashell transitions. The use of erbium complexes can provide significant advantages, i.e., strong ligand-centered absorption, and efficient and spatially homogeneous lanthanide-ion sensitization. Coordination complexes have also the necessary solubility to reach high concentrations (up to  $\sim 10^{20} \text{ cm}^{-3}$ ) in polymeric media without the drawback of concentration quenching. To date, very little is known about the response of these systems at high excitation fluences, where excited-state population saturation occurs; in particular, population inversion in Er<sup>III</sup> sensitized by molecular optical antennae has not yet been demonstrated.

In this letter we report on experimental assessment of infrared emission sensitization and emission saturation in model Er<sup>III</sup> coordination complexes with 8-quinolinolato (Q) and its dichloro-substitute as the organic ligands, photoexcited in the ligand absorption spectrum. We study the trimetallic complex Er<sub>3</sub>Q<sub>9</sub> and the partially halogenated, monometallic complex [Er(5,7ClQ)<sub>2</sub>(H5,7ClQ)<sub>2</sub>Cl] (H5,7ClQ = 5,7-dichloro-8-quinolinol; 5,7ClQ = deprotonated form of

H5,7ClQ), where Er<sup>III</sup> is coordinated to four ligands and one chloride (ErClQ<sub>4</sub>). Materials synthetic procedures, chemical, structural and photophysical characterization are described in recent reports.<sup>5,6</sup> The molecular structures of ErClQ<sub>4</sub> and Er<sub>3</sub>Q<sub>9</sub> are shown in Figure 1.

Linear optical measurements are performed to establish ligand-centered and ion-centered absorption strengths and emission spectra of erbium complexes. Ultraviolet–visible–infrared (UV–vis–IR) absorption cross-section and emission spectra are depicted in Figure 2. Cross-sections on the order of  $5 \times 10^{-17} \text{ cm}^2$  are found in both complexes for the ligand-centered absorption in the 350–380 nm wavelength range, while values of  $\sim 1 \times 10^{-20} \text{ cm}^2$  are measured for Er<sup>III</sup> absorption at the 1.54  $\mu\text{m}$  peak, relating to the <sup>4</sup>I<sub>15/2</sub> ↔ <sup>4</sup>I<sub>15/2</sub> transition manifold. Erbium lifetimes ( $\tau$ ),  $\sim 2 \mu\text{s}$  in both complexes (see Table 1), have been previously ascribed to nonradiative deactivation induced by C–H stretching vibrations.<sup>5,6</sup>

As a first step to determine Er<sup>III</sup> sensitization efficiency, we measure the quantum yields ( $\Phi_{\text{IR}}$ ) of the Er<sup>III</sup> IR emission by the relative method using tris(2,2′-bipyridyl)ruthenium(II) ion (Ru(bipy)<sub>3</sub><sup>2+</sup>;  $2.40 \times 10^{-3} \text{ M}$ ) in deaerated water as the reference standard ( $\Phi_{\text{R}} = 4.2\%$ ,  $\tau = 0.58 \mu\text{s}$ ).<sup>7</sup> The quantum yields is determined as

$$\Phi_{\text{IR}} = \frac{n_{\text{S(R)}}^2 I_{\text{S}} F_{\text{R}} A_{\text{R}}}{n_{\text{R}}^2 I_{\text{R}} F_{\text{S}} A_{\text{S}}} \Phi_{\text{R}}$$

where  $n_{\text{S(R)}}$  is the refractive index ( $n_{\text{DMSO}} = 1.4785$ ,  $n_{\text{H}_2\text{O}} = 1.333$ ),  $I_{\text{S(R)}}$  is the integrated emission rate (in photons/s),  $F_{\text{S(R)}}$  is the incident pump rate (in photons/s), and  $A_{\text{S(R)}}$  is the fraction of pump radiation absorbed in the sample,

**Received Date:** October 2, 2009

**Accepted Date:** November 4, 2009

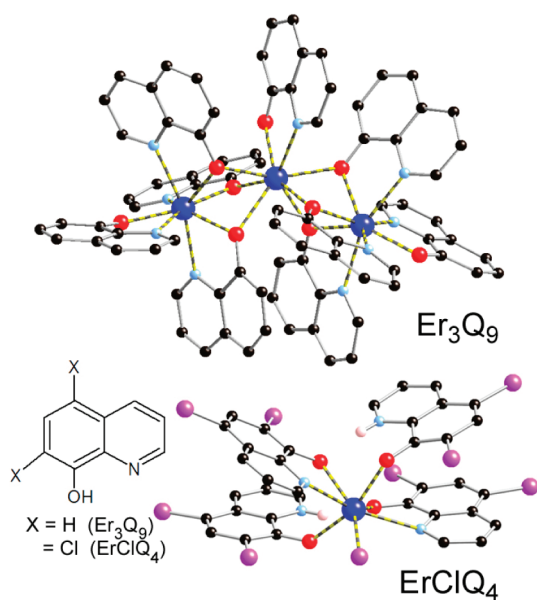


**Figure 1.** Molecular structures of monometallic  $\text{ErClQ}_4$  and trimetallic  $\text{Er}_3\text{Q}_9$ .

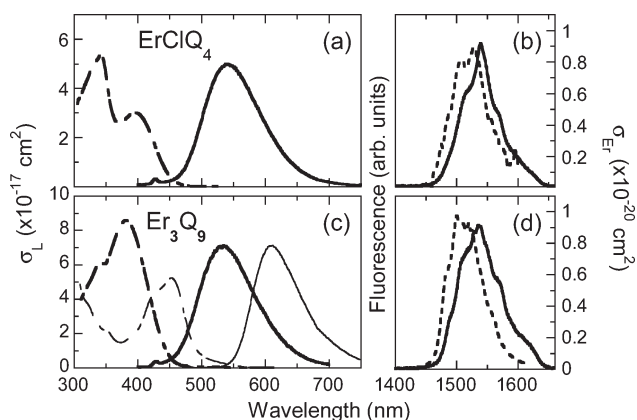


**Figure 2.** Absorption and emission spectra of  $\text{ErClQ}_4$  and  $\text{Er}_3\text{Q}_9$  in anhydrous dimethyl sulfoxide (DMSO) solutions. (a,c) Ligand-centered absorption cross-section ( $\sigma_L$ , dashed lines) and fluorescence intensity (solid lines) spectra. Thin lines refer to  $\text{Ru}(\text{bipy})_3^{2+}$  in deaerated water solution. (b,d)  $\text{Er}^{\text{III}}$ -centered absorption cross-section ( $\sigma_{\text{Er}}$ , dashed lines) and fluorescence spectra (solid lines) relating to the  $^4\text{I}_{13/2} \leftrightarrow ^4\text{I}_{15/2}$  transition manifold.

S (reference, R).  $I_{\text{S(R)}}$  is inferred from measured detector photocurrent using sample/reference-corrected emission spectra, filters' and collecting optics' transmittance spectra, and detector spectral responsivity. Experimental conditions ensure quasi-stationary operation at low excitation levels and negligible inner-filter effects in both sample and reference solutions.

Erbium sensitization efficiency ( $\eta_{\text{S}}$ ) is estimated from the equation  $\Phi_{\text{IR}} = \eta_{\text{S}} \cdot \tau \tau_{\text{rad}}$ , where  $\tau_{\text{rad}}$  is the  $\text{Er}^{\text{III}}$  radiative lifetime;  $\tau_{\text{rad}}$  is in turn determined from integrated absorption using Strickler–Berg formula:<sup>8</sup>

$$\tau_{\text{rad}} = 8\pi n^2 c \frac{1}{\langle \lambda^3 \rangle_1 g_u} \int \frac{\sigma_{\text{Er}}(\lambda)}{\lambda} d\lambda$$

**Table 1.** Photophysical Parameters of  $\text{Er}^{\text{III}}$  in  $\text{ErClQ}_4$  and  $\text{Er}_3\text{Q}_9$  in Anhydrous DMSO Solutions

compd	$\tau$ ( $\mu\text{s}$ )	$\tau_{\text{rad}}$ (ms)	$\Phi_{\text{IR}}$ (%)	$\eta_{\text{S}}$ (%)
$\text{ErClQ}_4$	2.15(10)	4.50(45)	$3.85(40) \times 10^{-2}$	80(16)
$\text{Er}_3\text{Q}_9$	2.20(10)	4.35(45)	$3.90(40) \times 10^{-2}$	77(15)

where  $n$  is the refractive index, and  $c$  is the speed of light;  $\langle \dots \rangle_1$  refers to the average over the corrected emission spectrum,  $g_{u(l)} = 2J_{u(l)} + 1$  is the upper(lower) manifold degeneracy, and  $\sigma_{\text{Er}}$  is the  $\text{Er}^{\text{III}}$  absorption cross-section.

Erbium radiative lifetime values ( $\sim 4.5$  ms) are found to lie within the range of literature data (0.66–14 ms),<sup>9</sup> and  $\text{Er}^{\text{III}}$  IR fluorescence sensitization is inferred to be very efficient, close to 80%, both in  $\text{ErClQ}_4$  and  $\text{Er}_3\text{Q}_9$ .<sup>10,11</sup> These results are consistent with theoretical predictions of ligand-to-erbium transfer rates at least 2 orders of magnitude higher than in the case of trivalent europium complexes.<sup>12</sup> Photophysical parameters of  $\text{Er}^{\text{III}}$  in  $\text{ErClQ}_4$  and  $\text{Er}_3\text{Q}_9$  complexes are summarized in Table 1.

With the aim of investigating  $\text{Er}^{\text{III}}$  excited-state population saturation, we perform high-excitation IR fluorescence measurements with subnanosecond pulse excitation. Experimental conditions are chosen so as to render excitation inhomogeneity and heating effects negligible. Absorption of the pump pulses does not saturate, and transmitted energy increases linearly with incident energy up to the highest fluences (hollow squares in Figure 3). Pump fluence is converted into excitation number ( $\mu$ ), i.e., the average number of photoexcitations that a pump pulse injects into the ligands of a single complex. Thus,  $\mu = \sigma_L \cdot D/h\nu$ , where  $\sigma_L$  is the ligand-centered absorption cross-section,  $D$  is the pulse fluence, and  $h\nu$  the pump photon energy.

Infrared emission intensity is proportional to the  $\text{Er}^{\text{III}}$  excited-state population,  $n$ . Intensity is thus translated into  $n$  upon data rescaling so as to fit data points to the line  $n(\mu) = \eta_{\text{S}} \cdot \mu$  at low excitation numbers ( $\mu < 0.1$ ). Experimental results are shown as the dots in Figure 3. Full dots relate to time-integrated IR emission intensity, while the empty dots (panel b) represent the initial amplitude of the IR fluorescence decay traces. Saturation is clearly observed at high excitation levels ( $\mu > 1$ ). We measure a moderate shortening of  $\text{Er}^{\text{III}}$  lifetime with increasing  $\mu$  ( $\sim 10\%$  across the 0.2–5 range), which only results in small overestimate of the saturation effect in the analysis with time-integrated data.

These results provide evidence for  $\text{Er}^{\text{III}}$  population saturation at around the inversion threshold ( $n = 0.5$ ) in monometallic  $\text{ErClQ}_4$ , while the  $n = 1.5$  threshold value is only approached in trimetallic  $\text{Er}_3\text{Q}_9$ . Experimental findings are compared to population saturation curves calculated for “ideal” monometallic and trimetallic erbium complexes. We assume that the number of ligand photoexcitations injected into a given complex followed Poissonian statistics, and introduce phase-space filling of the lanthanide-ion excited states as the only mechanism for saturation. Thus, only photoexcitations injected into the ligand in excess to the number of  $\text{Er}^{\text{III}}$  ions of the complex decay or annihilate before they can contribute to IR emission. Consequently,  $\text{Er}^{\text{III}}$  sensitization efficiency is taken equal to unity for unexcited ions

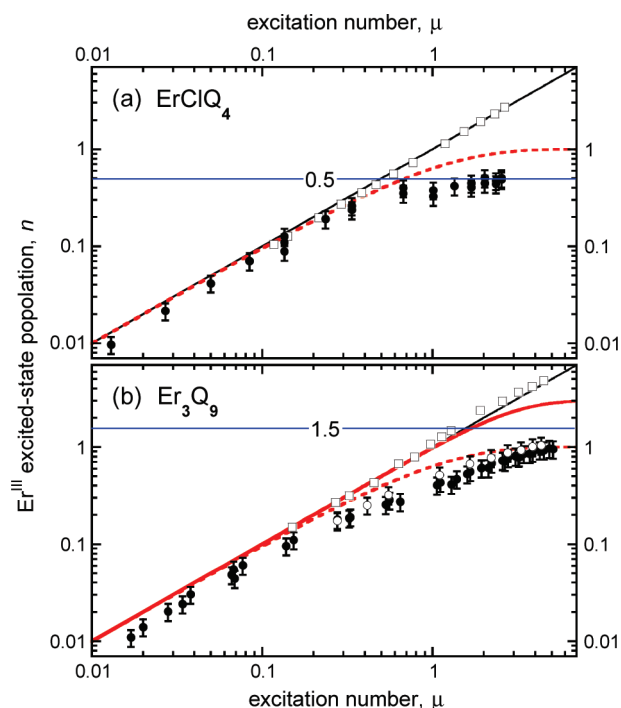


**Figure 3.** Dots:  $\text{Er}^{\text{III}}$  excited-state population ( $n$ ) inferred in  $\text{Er}_3\text{Q}_9$  (a) and  $\text{ErClQ}_4$  (b) versus excitation number ( $\mu$ ) with subnanosecond excitation. Filled (open) dots relate to time-integrated (time-resolved) IR fluorescence data. Open squares: Energy of transmitted pump pulses normalized to overlay the identity function [ $n(\mu) = \mu$ , thin solid line]. Curves: model calculations of  $\text{Er}^{\text{III}}$  excited-state population versus  $\mu$  for a monometallic complex ( $n_1$ , dashed red curves) and trimetallic complex ( $n_3$ , solid red curve). Horizontal lines mark the  $\text{Er}^{\text{III}}$  population inversion threshold.

and zero for excited ones. Model curves are then described by the equation

$$n_m(\mu) = \sum_{k < m} k \cdot P_\mu(k) + m \cdot \sum_{k \geq m} P_\mu(k)$$

where  $m$  is the number of  $\text{Er}^{\text{III}}$  ions per complex, and  $P_m(k) = \mu^k \cdot e^{-\mu}/k!$ . Clearly,  $n_m(\mu)$  tends to  $m$  for large values of  $\mu$ . The  $n_1(\mu)$  and  $n_3(\mu)$  curves are also shown in Figure 3. Model curves underestimate the experimental saturation trends, suggesting that additional excited-state losses, not included in the phase-space filling model, should be taken into account. We mention here two examples: (i) In trimetallic complexes, model curve  $n_3(\mu)$  neglects two-excitation and three-excitation annihilations; this mechanism could reduce erbium occupation to values lower than the phase-space filling limit ( $n = 3$ ). (ii) The process of excitation-excitation annihilation always ends up with the complex in a high-energy state, in which the lanthanide is possibly in the oxidized form,  $\text{Er}^{\text{IV}}$ , with consequent reduction of average erbium sensitization efficiency.<sup>13</sup>

Finally, we estimate the pump intensity necessary to reach  $\text{Er}^{\text{III}}$  population inversion under steady-state operation. Continuous wave (cw) threshold intensity ( $I_{\text{th}}$ ) can be derived from threshold excitation number ( $\mu_{\text{th}}$ ) or threshold pump fluence ( $D_{\text{th}}$ ) measured in the pulsed regime using the relation  $I_{\text{th}} = D_{\text{th}}/\tau = \mu_{\text{th}} h\nu/\sigma_L \eta_S \tau$ . Given  $\mu_{\text{th}} \approx 1$ ,  $I_{\text{th}}$  turns out to be  $\sim 9 \text{ kW/cm}^2$ . Recently, halogenation of the ligands and dispersion

of the complexes in IR transmitting media, e.g., perfluorinated polymers, has been shown to be effective in reducing vibrational quenching induced by C–H groups, with consequent increase in  $\text{Er}^{\text{III}}$  lifetime by 2 orders of magnitude.<sup>14–16</sup> If  $\tau$  reached the radiative limit, threshold pump intensity would be decreased to values less than  $5 \text{ W/cm}^2$  that are practical for indirect pumping by semiconductor light-emitting diodes.<sup>17</sup>

In conclusion, we show experimental evidence for transient  $\text{Er}^{\text{III}}$  population saturation near inversion threshold in a monometallic coordination complex exhibiting very efficient lanthanide-ion sensitization. Our results could be translated to the solid state by complex incorporation in transparent polymer or glass matrices. Efficient  $\text{Er}^{\text{III}}$  sensitization by organic molecular antennae in suitable coordination complexes holds potential for the development of novel gain media at IR telecom wavelengths.

## Experimental Section

Anhydrous DMSO solutions of the complexes are used in quartz cuvettes for optical measurements. UV–vis–IR absorbance spectra are recorded on  $\sim 10^{-3} \text{ mol dm}^{-3}$  (M) solutions using a cw photospectrometer. Diluted solutions ( $\sim 10^{-5} \text{ M}$ ) are used for vis fluorescence measurements in a cw spectrofluorimeter with excitation at 380 nm; IR fluorescence spectra are measured upon ligand excitation at 392 nm by frequency-doubled subpicosecond output pulses of a Ti:Sapphire regenerative amplifier with a 1 kHz repetition rate, using a spectrograph equipped with a one-dimensional InGaAs charge-coupled detector. vis–IR fluorescence spectra are corrected for instrument response functions. IR fluorescence decay transients are taken with a fast InGaAs amplified photodiode.

$\text{Er}^{\text{III}}$  IR emission quantum yields are measured in  $2.40 \times 10^{-3} \text{ M}$  ( $8.63 \times 10^{-4} \text{ M}$ ) solution of  $\text{ErClQ}_4$  ( $\text{Er}_3\text{Q}_9$ ) excited at 380 nm by frequency-doubled subpicosecond pulses from a Ti:Sapphire oscillator operating at 82 MHz repetition rate. Sample solution absorbances (i.e., optical density  $\text{OD}_S$ ) at pump wavelength are 1.70 ( $\text{ErClQ}_4$ ) and 1.93 ( $\text{Er}_3\text{Q}_9$ ). IR emission is collected using back-reflection geometry, passed through long-wavelength filters to cut UV–vis radiation, and detected with a large-area Ge photodiode. The reference sample solution (quantum yield standard) is excited at 410 nm ( $\text{OD}_R = 1.86$ ), and the metal-centered emission peaked at  $\approx 600 \text{ nm}$  is detected upon change of the Ge photodiode with a large-area Si photodiode.

High-excitation IR fluorescence experiments are performed using a passively Q-switched powerchip laser emitting 310-ps-long pulses at 355 nm with 120 Hz repetition frequency. Pulse fluences up to  $55 \text{ mJ/cm}^2$  are used to excite diluted solutions of the complexes ( $\text{OD}_S \sim 0.2$ ). Spatial filtering of the emission is adopted prior to signal detection. Other experimental conditions are the same as for the IR quantum yield measurements.

## AUTHOR INFORMATION

### Corresponding Author:

\*To whom correspondence should be addressed. Tel: +39-070-6758483. Fax: +39-070-510171. E-mail: francesco.quochi@dsf.unica.it.

**ACKNOWLEDGMENT** Work in Cagliari was partially funded by MIUR through FIRB projects (Synergy-FIRBRNE03S7XZ and FIRB-RBAU01N449). Work in Cagliari and Groningen was partially funded by the European Commission through the Human Potential Programs (RTN Nanomatch, Contract No. MRTN-CT-2006-035884). The authors thank A. Cardini for providing the powerchip laser, and G. Mula, S. Setzu, and T. Pivetta for assistance on spectrophotometric and spectrofluorimetric measurements. M.S. acknowledges the Italian Government Program "Rientro dei Cervelli". F.A. is indebted to the "Fondazione Banco di Sardegna" for financial support.

## REFERENCES

- Eldada, L.; Shacklette, L. W. Advances in Polymer Integrated Optics. *IEEE J. Sel. Top. Quantum Electron.* **2000**, *6*, 54–68.
- Gillin, W. P.; Curry, R. J. 1.54  $\mu\text{m}$  Erbium (III) Tris(8-hydroxyquinoline) ( $\text{ErQ}$ ): A Potential Material for Silicon Compatible 1.5  $\mu\text{m}$  Emitters. *Appl. Phys. Lett.* **1999**, *74*, 798–800.
- Kuriki, K.; Koike, Y.; Okamoto, Y. Plastic Optical Fiber Lasers and Amplifiers Containing Lanthanide Complexes. *Chem. Rev.* **2002**, *102*, 2347–2356.
- Polman, A.; van Veggel, F. C. J. M. Broadband Sensitizers for Erbium-Doped Planar Optical Amplifiers: Review. *J. Opt. Soc. Am. B* **2004**, *21*, 871–892.
- Artizzu, F.; Deplano, P.; Marchi, L.; Mercuri, M. L.; Pilia, L.; Serpe, A.; Quochi, F.; Orrù, R.; Cordella, F.; Meinardi, F.; et al. Structure and Emission Properties of  $\text{Er}_3\text{Q}_9$  ( $\text{Q}$  = 8-quinolinate). *Inorg. Chem.* **2005**, *44*, 840–842.
- Artizzu, F.; Marchi, L.; Mercuri, M. L.; Pilia, L.; Serpe, A.; Quochi, F.; Orrù, R.; Cordella, F.; Saba, M.; Mura, A.; et al. New Insights on Near-Infrared Emitters Based on Er-quinolinate Complexes: Synthesis, Characterization, Structural and Photophysical Properties. *Adv. Funct. Mater.* **2007**, *17*, 2365–2376.
- Werts, M. H. V.; Jukes, R. T. F.; Verhoeven, J. W. The Emission Spectrum and the Radiative Lifetime of  $\text{Eu}^{3+}$  in Luminescent Lanthanide Complexes. *Phys. Chem. Chem. Phys.* **2002**, *4*, 1542–1548.
- Strickler, S. J.; Berg, R. A. Relationship between Absorption Intensity and Fluorescence Lifetime of Molecules. *J. Chem. Phys.* **1962**, *37*, 814–822. The formula is rewritten as a function of the integrated absorption cross-section.
- Nonat, A.; Imbert, D.; Pécaut, J.; Giraud, M.; Mazzanti, M. Structural and Photophysical Studies of Highly Stable Lanthanide Complexes of Tripodal 8-Hydroxyquinolinate Ligands Based on 1,4,7-Triazacyclononane. *Inorg. Chem.* **2009**, *48*, 4207–4218.
- Literature data for the  $\eta_{\text{S}}$  range from less than 1 % ( $\tau_{\text{rad}} = 0.66 \text{ ms}^9$ ) to ~50 % (assuming  $\tau_{\text{rad}} = 5 \text{ ms}$ ): Albrecht, M.; Osetska, O.; Klankermayer, J.; Fröhlich, R.; Gumy, F.; Bünzli, J.-C. G. Enhancement of Near-IR Emission by Bromine Substitution in Lanthanide Complexes with 2-Carboxamide-8-Hydroxyquinoline. *Chem. Commun.* **2007**, 1834–1836.
- The high values found for erbium sensitization efficiency have been confirmed by the results of recent studies on the excited-state temporal dynamics. Time-resolved studies will be the subject of a future paper.
- Malta, O. L. Mechanisms of Non-Radiative Energy Transfer Involving Lanthanide Ions Revisited. *J. Non-Cryst. Solids* **2008**, *354*, 4770–4776.
- Horrocks, W. D.; Bolender, J. P.; Smith, W. D.; Supkowski, R. M. Photosensitized Near Infrared Luminescence of Ytterbium(III) in Proteins and Complexes Occurs via an Internal Redox Process. *J. Am. Chem. Soc.* **1997**, *119*, 5972–5973.
- Mancino, G.; Ferguson, A. J.; Beeby, A.; Long, N. J.; Jones, T. S. Dramatic Increases in the Lifetime of the  $\text{Er}^{3+}$  Ion in a Molecular Complex Using a Perfluorinated Imidodiphosphinate Sensitizing Ligand. *J. Am. Chem. Soc.* **2005**, *127*, 524–525.
- Tan, R. H. C.; Pearson, J. M.; Zheng, Y.; Wyatt, P. B.; Gillin, W. P. Evidence for Erbium–Erbium Energy Migration in Erbium(III) Bis(perfluoro-p-tolyl)phosphinate. *Appl. Phys. Lett.* **2008**, *92*, 103303.
- Quochi, F.; Orrù, R.; Cordella, F.; Mura, A.; Bongiovanni, G.; Artizzu, F.; Deplano, P.; Mercuri, M. L.; Pilia, L.; Serpe, A. Near Infrared Light Emission Quenching in Organolanthanide Complexes. *J. Appl. Phys.* **2006**, *99*, 053520.
- Yang, Y.; Turnbull, G. A.; Samuel, I. D. W. Hybrid Optoelectronics: A Polymer Laser Pumped by a Nitride Light-Emitting Diode. *Appl. Phys. Lett.* **2008**, *92*, 163306.